galaxies

MDPI

Article

First Results from a Panchromatic HST/WFC3 Imaging Study of the Young, Rapidly Evolving Planetary Nebulae NGC 7027 and NGC 6302

Joel H. Kastner [1,2,*], Jesse Bublitz [2], Bruce Balick [3], Rodolfo Montez, Jr. [4], Adam Frank [5] and Eric Blackman [5]

1 Center for Imaging Science and Laboratory for Multiwavelength Astrophysics, Rochester Institute of Technology, Rochester, NY 14623, USA
2 School of Physics & Astronomy, Rochester Institute of Technology, Rochester, NY 14623, USA; jtb1435@rit.edu
3 Department of Astronomy, University of Washington, Seattle, WA 98195, USA; balick@uw.edu
4 Center for Astrophysics | Harvard & Smithsonian, Cambridge, MA 02138, USA; rodolfo.montez@cfa.harvard.edu
5 Department of Physics & Astronomy, University of Rochester, Rochester, NY 14627, USA; afrank@pas.rochester.edu (A.F.); blackman@pas.rochester.edu (E.B.)
* Correspondence: jhk@cis.rit.edu

Received: 2 March 2020; Accepted: 10 May 2020; Published: 15 June 2020

Abstract: We present the first results from comprehensive, near-UV-to-near-IR Hubble Space Telescope Wide Field Camera 3 (WFC3) emission-line imaging studies of two young planetary nebulae (PNe), NGC 7027 and NGC 6302. These two objects represent key sources for purposes of understanding PNe shaping processes. Both nebulae feature axisymmetric and point-symmetric (bipolar) structures and, despite hot central stars and high nebular excitation states, both harbor large masses of molecular gas and dust. The sweeping wavelength coverage of our Cycle 27 Hubble Space Telescope (HST)/WFC3 imaging surveys targeting these two rapidly evolving PNe will provide a battery of essential tests for theories describing the structural and chemical evolution of evolved star ejecta. Here, we present initial color overlays for selected images, and we highlight some of the first results gleaned from the surveys.

Keywords: stars—evolution; stars—winds and outflows; planetary nebulae

1. Introduction

The transformation from slow (∼10–20 km s^{-1}), quasi-spherical asymptotic giant branch (AGB) star wind to fast (∼100–300 km s^{-1}), collimated outflows during post-AGB and early planetary nebula (PN) evolutionary stages remains one of the most intriguing yet poorly understood aspects of the deaths of intermediate-mass stars. The community of PN researchers has reached a broad consensus that the influence of a companion to the mass-losing central star is responsible for this transformation (e.g., [1–3]), and that the interaction of collimated post-AGB outflows with previously ejected AGB wind material can explain the shapes of PNe spanning a wide range of morphologies and dynamical ages (e.g., [4,5]). As discussions at the WorkPlaNS II meeting made apparent, however, fundamental problems raised by this general binary-driven PNe shaping scenario remain to be resolved. Among the most vexing challenges is to specify the nature of the binary interactions underlying the late-breaking (post-AGB, pre-PNe) collimated flows: are such outflows generated via onset of a common envelope (CE) configuration, jets associated with a companion star's accretion disk, or some combination of these (or other) potential mass ejection and collimation mechanisms (see, e.g., [6])?

Our understanding of this PNe shaping process has benefitted enormously from Hubble Space Telescope (HST) imaging of PNe and pre-PNe in a plethora of optical and near-IR emission lines (e.g., [4,7–10]). Yet—even as HST passed a quarter century of unparalleled achievements in the realm of subarcsecond imaging of astrophysical sources—the tremendous potential of its Wide Field Camera 3 (WFC3) to obtain a comprehensive set of emission-line images extending over its full wavelength range, from near-UV through optical through near-IR, had yet to be exploited for any individual PN. This gaping hole in HST's legacy extended to even the most intensively studied, structurally rich PNe that serve as touchstones to understand PNe shaping, photoionization, and shock processes.

With this as motivation, we have undertaken the first such comprehensive NUV-to-NIR HST/WFC3 emission-line studies of two seminal, young, and (evidently) rapidly evolving PNe: (1) the enigmatic NGC 7027($D \sim 0.9$ kpc [11], dynamical age ∼1100–1600 yr [9]), which for decades has served as the "industry standard" for astrophysical emission-line and continuum studies from radio through X-ray regimes (e.g., [12,13]); and (2) the extreme bipolar nebula NGC 6302 ($D \sim 1.2$ kpc, dynamical age $\sim$ 2200 yr; [14]), which was among the most photogenic subjects for early science observations with WFC3 upon its installation in HST in 2009. These two structurally complex PNe have been proposed as representative of the two distinct classes of interacting-binary-derived PNe shaping process noted earlier, i.e., CE (NGC 7027; e.g., [13]) and companion accretion disk (NGC 6302; e.g., [15]). Both PNe are (likely) descended from relatively high-mass (∼3–5 $M_{\odot}$) progenitors; both display among the highest known states of ionization and excitation among PNe, indicative of exceedingly hot central stars ($T_{eff} \sim 200$ kK; [10,16]). Both have axisymmetric and point-symmetric (bipolar) structures and, despite their high nebular excitation and high-T_{eff} central stars, harbor large masses of molecular gas and dust (e.g., [12,15,17] and refs. therein). Indeed, given the enormous estimated mass of its molecular torus (∼1 $M_{\odot}$) [18], it is also possible that the central star of NGC 6302 has emerged from a CE event that took place within the past few hundred years (given the dynamical age of the nebula). On the other hand, in contrast to NGC 7027, NGC 6302 does not display X-ray emission from shocks [19]. Thus, NGC 6302 may represent a snapshot of PNe evolution in which nebula-shaping "blowouts," such as characterize present-day NGC 7027 [20], have very recently expanded and cooled below (X-ray) detectability.

In this paper—summarizing a poster presented during the WORKPLANS II meeting [21]—we highlight some of the first results gleaned from our HST/WFC3 imaging surveys of NGC 7027 and NGC 6302.

2. Observations

2.1. Survey Strategy and Goals

In Table 1, we summarize our HST/WFC3 imaging program targeting NGC 7027 and NGC 6302 (Program ID 15953; PI: J. Kastner) in terms of overarching science goals, filters used, and the specific lines, atomic/ionic species, and bands targeted. In the following, we briefly describe the main components of this observing strategy.

Table 1. Hubble Space Telescope (HST)/Wide Field Camera 3 (WFC3) Imaging Survey of NGC 7027 and NGC 6302: Overview.

Science Goal	λ Regime: WFC3 Filters [a]	Lines/Bands Targeted
photoionization vs. heat conduction	near-UV: FQ243N, F343N	[Ne IV], [Ne V]
shocks vs. photoionization	visible: F487N, F502N, F656N, F673N	Hβ, [O III], Hα, [S II]
shocks vs. photoionization	near-IR: F128N, F130N, F164N, F167N	Paβ, [Fe II] (+ adj. continuum)
scattered light dust imaging	near-IR: F110W, F160W	'J', 'H' band continuum

Note: ([a]) For NGC 6302, we also obtained an image in filter F658N ([N II]).

Mapping variations in PNe ionization state, via imaging in lines of highly ionized Ne. Both nebulae were imaged using narrow-band near-UV filters that isolate emission from forbidden transitions of adjacent

ionization states of Ne (specifically, [Ne IV] λ2425 and [Ne V] λ3426). The resulting Ne ionization state maps can be used to establish the illumination patterns and penetration depths of nebular gas by EUV photons from the unusually hot central stars within NGC 7027 and NGC 6302. In the case of NGC 7027, the [Ne IV] and [Ne V] imaging was also aimed at the possible detection of conduction fronts at the interfaces between $\sim 10^4$ K nebular gas and $\sim 10^6$ K, X-ray-emitting plasma generated by highly energetic shocks [20].

Establishing the domain of shocks and dust, via near-IR imaging. The [Fe II] emission line at 1.64 μm is a well-established tracer of moderate-strength ($\sim$100 km s^{-1}) astrophysical shocks (e.g., [22]). In PNe, such emission typically arises where stellar wind streamlines slam into the the walls of bipolar cavities, creating an inner (reverse) shock that should vary with polar angle (since only the perpendicular velocity component shocks the gas). The H_2 emission that is a ubiquitous feature of bipolar PNe like NGC 7027 and NGC 6302 [23] can arise from slower ($\sim$20 km s^{-1}), leading shocks; indeed, the combination of [Fe II] and H_2 emission has been vital in diagnosing shocks in YSO outflows (e.g., [24]). The dust structures in both nebulae, and the potential influence of these structures on shock-induced nebular shaping, will be further explored via near-IR continuum (scattered-light) imaging.

Connecting UV/NIR-based and optical-based photoionization and shock diagnostics. Maps of various line ratios constructed from images of [O III] 5007 Å, [S II] 6716, 6731 Å, Hα, and Hβ emission, when placed in the context of model predictions, have long served to disentangle shock- vs. UV-driven excitation and ionization (e.g., [25] and refs. therein). In obtaining a suite of images in these bright emission lines, we can further exploit the aforementioned combination of [Ne V]/[Ne IV] and [Fe II] imaging to cross-calibrate these (near-UV and near-IR) diagnostics of shock-induced ionization vs. photoionization against (far more widely used) optical emission-line diagnostics.

2.2. Image Acquisition and Processing

Data for our HST/WFC3 imaging surveys of NGC 7027 and NGC 6302 were obtained early in Cycle 27 (2019 September and October) during the course of 11 orbits[1]. Typical total exposure times were $\sim$1200 s. Images presented in this overview paper have thus far only been subject to standard WFC3 pipeline processing. Refinement of processing parameters, in particular cosmic ray removal and optimizing astrometric accuracy and precision (absolute reference frame and filter-to-filter image registration), is now underway.

3. First Results

Color overlays of selected narrow-band WFC3 images of NGC 7027 and NGC 6302 spanning the near-UV through near-IR wavelength ranges are presented in Figures 1 and 2, respectively. Below, we briefly highlight some of the first results obtained from these and the other WFC3 images of each nebula.

3.1. NGC 7027

In Figure 1, NGC 7027 displays the now-familiar juxtaposition of structures previously seen in HST imaging [9,10]: a bright, well-defined elliptical shell of semimajor axis $\sim 6''$ ($\sim 8 \times 10^{16}$ cm) surrounded by a set of concentric circular rings extending to at least $\sim 15''$ ($\sim 2 \times 10^{17}$ cm) in radius; a narrow equatorial dust ring or torus skirting the elliptical shell's minor axis; and a complex set of multipolar "blowouts," oriented more or less along the elliptical shell's major axis, that appear to puncture the shell and project well out into the concentric ring system. The dust rings are seen in reflection and, because they are illuminated by NGC 7027's inner, highly ionized shell—which is among

[1] Initial observations of NGC 6302 in filters F502N and F673N failed, and so were repeated during 2 orbits in 2020 March, with the addition of filter F658N.

the brightest [O III] sources in the sky—they appear greenish in Figure 1 (i.e., they are brightest in the F502N image). The new WFC3 images also reveal, in unprecedented detail, the delicate, filamentary dust structures that are superimposed on the elliptical shell. These dust filaments, which appear to be associated (perhaps entrained within) the multipolar blowout structures, appear red in Figure 1 (i.e., they are brightest in the F164N image) largely as a consequence of their large local extinction, not because they are regions of bright [Fe II] line emission. The same is true of the dusty equatorial ring. A preliminary F164N−F167N difference image (not shown) reveals that, in fact, the [Fe II] emission traces the southeast-northwest-oriented collimated outflows that also produce the X-ray-emitting shocks imaged by Chandra [20]. The possible presence of bright [Ne V] emission in the northwest blowout (the bluest region of Figure 1) could be due to heat conduction from the X-ray-emitting shocked wind plasma to the cooler, photoionized nebular gas. However, this and other extended blue regions of Figure 1 may instead be due to bright, interior nebular line emission that is scattered off dust in NGC 7027's extended, cool (predominantly neutral/molecular) envelope. Finally, we note that the central star is detected in most of our new WFC3 images, such that we should now be able to construct (and attempt to deredden) the star's spectral energy distribution from 243 nm to 1.6 μm.

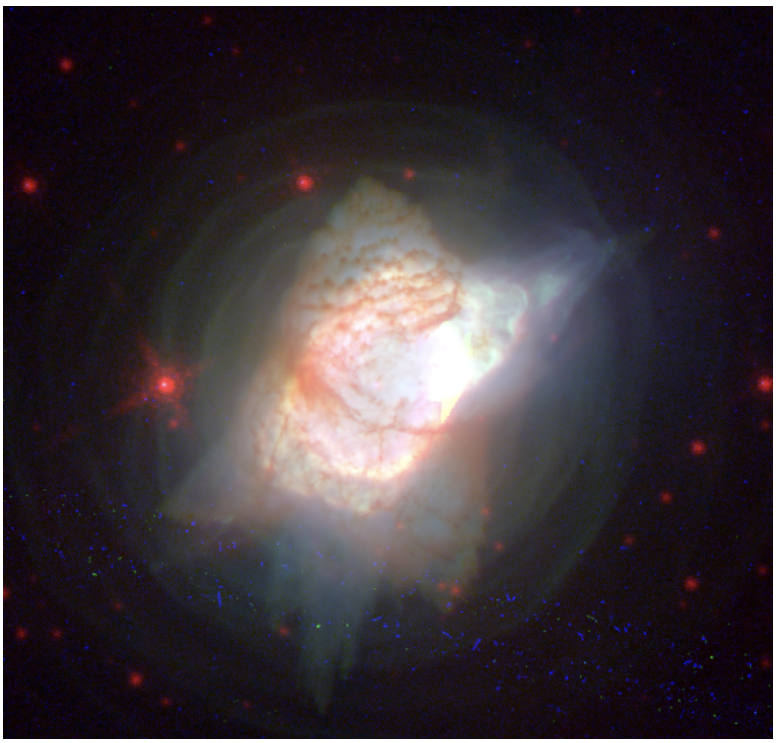

Figure 1. Color overlay of Cycle 27 HST/WFC3 narrow-band images of NGC 7027. Filter F343N ([Ne V]) is blue, F502N ([O III]) is green, and F164N ([Fe II]) is red. The field of view is $\sim 38'' \times 38''$; north is up and east is to the left.

3.2. NGC 6302

In Figure 2, NGC 6302 displays its classical, pinched-waist bipolar morphology. As in the images previously obtained by HST [18,26], the new WFC3 images clearly define the thick, dusty toroidal equatorial structure (central dark lane) that bisects the polar lobes, and reveal fine structures (knots and filaments) within the lobes. The most striking aspect of this new WFC3 color image overlay is the bright, S-shaped [Fe II] emission (red channel, i.e., F164N filter, in Figure 2) that traces the southern interior of the east lobe rim and the northern interior of the west lobe rim, in point-symmetric fashion. Given that [Fe II] emission is typically a marker of fast shocks, the strict confinement of the emission to these point-symmetric lobe structures strongly suggests that these particular surfaces of the PNe lobes

are being actively shaped by collimated winds emanating from the immediate vicinity of its central star. This surprising misalignment of the central engine's present collimated fast wind direction and the nebula's main axis of symmetry presents an especially daunting challenge for models of the origin and evolution of NGC 6302's bipolar structure. The central star itself appears to be directly detected, within the dark lane, in our new near-IR (F128N and F164N) WFC3 images. However, we find this star is offset by $\sim$0.1–0.2″ from the point-like source that was identified as the PN's central star in the first-epoch (2009) WFC3 images [26]. Followup astrometry is underway, to confirm whether these putative central star identifications are in fact discrepant.

Figure 2. Color overlay of Cycle 27 HST/WFC3 narrow-band images of NGC 6302. Filter F343N ([Ne V]) is blue, F128N (Paβ) is green, and F164N ([Fe II]) is red. The field of view is $\sim$120″ × 70″; north is up and east is to the left.

Author Contributions: Conceptualization, J.H.K., B.B., J.B., R.M.J.; methodology, J.H.K., B.B., R.M.J., A.F., and E.B.; formal analysis, J.H.K., B.B., J.B., and R.M.J.; investigation, J.H.K. and B.B.; data curation, J.H.K., J.B., and R.M.J.; writing—original draft preparation, J.H.K.; writing—review and editing, J.H.K., B.B., J.B., and E.B.; visualization, J.H.K.; supervision, J.H.K.; project administration, J.H.K.; funding acquisition, J.H.K. All authors have read and agreed to the published version of the manuscript.

Funding: This research is funded by Space Telescope Science Institute grant number HST-GO-15953.001.

Conflicts of Interest: The authors declare no conflicts of interest.

References

1. Akashi, M.; Bear, E.; Soker, N. Forming H-shaped and barrel-shaped nebulae with interacting jets. *Mon. Not. R. Astron. Soc.* **2018**, *475*, 4794–4808. [CrossRef]
2. Frank, A.; Chen, Z.; Reichardt, T.; De Marco, O.; Blackman, E.; Nordhaus, J. Planetary Nebulae Shaped by Common Envelope Evolution. *Galaxies* **2018**, *6*, 113. [CrossRef]
3. Hillwig, T. Surveying Planetary Nebulae Central Stars for Close Binaries: Constraining Evolution of Central Stars Based on Binary Parameters. *Galaxies* **2018**, *6*, 85. [CrossRef]
4. Balick, B.; Frank, A.; Liu, B. Models of the Mass-ejection Histories of Pre-planetary Nebulae. III. The Shaping of Lobes by Post-AGB Winds. *Astrophys. J.* **2019**, *877*, 30. [CrossRef]
5. Huarte-Espinosa, M.; Frank, A.; Balick, B.; Blackman, E.G.; De Marco, O.; Kastner, J.H.; Sahai, R. From bipolar to elliptical: Simulating the morphological evolution of planetary nebulae. *Mon. Not. R. Astron. Soc.* **2012**, *424*, 2055–2068. [CrossRef]

6. Soker, N. Shaping planetary nebulae with jets and the grazing envelope evolution. *Galaxies* **2020**, *8*, 26. [CrossRef]
7. Balick, B.; Frank, A.; Liu, B.; Corradi, R. Models of the Mass-ejection Histories of Pre-planetary Nebulae. II. The Formation of Minkowski's Butterfly and its Proboscis in M2–9. *Astrophys. J.* **2018**, *853*, 168. [CrossRef]
8. Sahai, R.; Trauger, J.T. Multipolar bubbles and jets in low-excitation planetary nebulae: Toward a new understanding of the formation and shaping of planetary nebulae. *Astron. J.* **1998**, *116*, 1357. [CrossRef]
9. Schönberner, D.; Balick, B.; Jacob, R. Expansion patterns and parallaxes for planetary nebulae. *Astron. Astrophys.* **2018**, *609*, A126. [CrossRef]
10. Latter, W.B, Dayal, A.; Bieging, J.H.; Meakin, C.; Hora, J.L.; Kelly, D.M.; Tielens, A.G. Revealing the photodissociation region: HST/NICMOS imaging of NGC 7027. *Astrophys. J.* **2000**, *539*, 783. [CrossRef]
11. Masson, C.R. The structure of NGC 7027 and a determination of its distance by measurement of proper motions. *Astrophys. J.* **1989**, *336*, 294–303. [CrossRef]
12. Bublitz, J.; Kastner, J.H, Santander-García, M.; Bujarrabal, V.; Alcolea, J.; Montez, R. A new radio molecular line survey of planetary nebulae-HNC/HCN as a diagnostic of ultraviolet irradiation. *Astron. Astrophys.* **2019**, *625*, A101. [CrossRef]
13. Kastner, J.H. X-Ray Imaging Spectroscopy of Planetary Nebulae in the Chandra/XMM Era: New Insight into Stellar Jets. *Astrophys. Space Sci. Proc.* **2009**, *13*, 367.
14. Meaburn, J.; Lloyd, M.; Vaytet, N.M H.; López, J.A. Hubble-type outflows of the high-excitation poly-polar planetary nebula NGC 6302–from expansion proper motions. *Mon. Not. R. Astron. Soc.* **2008**, *385*, 269–273. [CrossRef]
15. Santander-García, M.; Bujarrabal, V.; Alcolea, J.; Castro-Carrizo, A.; Contreras, C.S.; Quintana-Lacaci, G.; Corradi, R.L.; Neri, R. ALMA high spatial resolution observations of the dense molecular region of NGC 6302. *Astron. Astrophys.* **2017**, *597*, A27. [CrossRef] [PubMed]
16. Wright, N.J.; Barlow, M.J.; Ercolano, B.; Rauch, T. A 3D photoionization model of the extreme planetary nebula NGC 6302. *Mon. Not. R. Astron. Soc.* **2011**, *418*, 370–389. [CrossRef]
17. Bachiller, R.; Forveille, T.; Huggins, P.J.; Cox, P. The chemical evolution of planetary nebulae. *Astron. Astrophys.* **1997**, *324*, 1123–1134.
18. Matsuura, M.; Zijlstra, A.A.; Molster, F.J.; Waters, L.B.; Nomura, H.; Sahai, R.; Hoare, M.G. The dark lane of the planetary nebula NGC 6302. *Mon. Not. R. Astron. Soc.* **2005**, *359*, 383–400. [CrossRef]
19. Kastner, J.H.; Montez, R., Jr.; Balick, B.; Frew, D.J.; Miszalski, B.; Sahai, R.; Blackman, E.; Chu, Y.H.; De Marco, O.; Frank, A.; et al. The CHANDRA X-ray survey of planetary nebulae (ChanPlaNS): Probing binarity, magnetic fields, and wind collisions. *Astron. J.* **2012**, *144*, 58. [CrossRef]
20. Montez, R., Jr.; Kastner, J.H. Dissecting the X-Ray Emission in the Young Planetary Nebula NGC 7027. *Astrophys. J.* **2018**, *861*, 45. [CrossRef]
21. Aleman, I.; Bernard-Salas, J.; Kastner, J.H, Ueta, T.; Villaver, E. WORKPLANS: Workshop on Planetary Nebula Observations. *Galaxies* **2020**, *8*, 23. [CrossRef]
22. Barbosa, F.K.B.; Storchi-Bergmann, T.; McGregor, P.; Vale, T.B.; Rogemar Riffel, A. Modelling the [Fe ii] λ 1.644 μm outflow and comparison with H_2 and H^+ kinematics in the inner 200 pc of NGC 1068. *Mon. Not. R. Astron. Soc.* **2014**, *445*, 2353–2370. [CrossRef]
23. Kastner, J.H.; Weintraub, D.A.; Gatley, I.; Merrill, K.M.; Probst, R.G. H2 Emission from Planetary Nebulae: Signpost of Bipolar Structure. *Astrophys. J.* **1996**, *462*, 777. [CrossRef]
24. Youngblood, A.; Ginsburg, A.; Bally, J. The Orion Fingers: Near-IR Spectral Imaging of an Explosive Outflow. *Astron. J.* **2016**, *151*, 173. [CrossRef]
25. Danehkar, A.; Karovska, M.; Maksym, W.P.; Montez, R., Jr. Mapping Excitation in the Inner Regions of the Planetary Nebula NGC 5189 Using HST WFC3 Imaging. *Astrophys. J.* **2018**, *852*, 87. [CrossRef]
26. Szyszka, C.; Walsh, J.R.; Zijlstra, A.A.; Tsamis, Y.G. Detection of the Central Star of the Planetary Nebula NGC 6302. *Astrophys. J. Lett.* **2009**, *707*, L32. [CrossRef]